Magnetic polarons in antiferromagnetic $CaMnO_{3-x}$ ($x<0.01$) probed by ^{17}O NMR

A. Trokiner,[1] S. Verkhovskii,[1,2] A. Yakubovskii,[1,3] A. Gerashenko,[1,2] P. Monod,[1] K. Kumagai,[4] K. Mikhalev,[2] A. Buzlukov,[2] Z. Litvinova,[2] O. Gorbenko,[5] A. Kaul,[5] and M. Kartavtzeva[5]

[1]*Laboratoire de Physique du Solide, LPEM UPR5, CNRS, E.S.P.C.I., Paris 75231, France*

[2]*Institute of Metal Physics, Ural Branch of Russian Academy of Sciences, Ekaterinburg 620041, Russia*

[3]*Russian Research Centre "Kurchatov Institute", Moscow 123182, Russia*

[4]*Division of Physics, Graduate School of Sciences, Hokkaido University, Sapporo 060-0810, Japan*

[5]*Department of Chemistry, Moscow State University, Moscow 119991, Russia*

(Received 7 February 2009; revised manuscript received 12 May 2009; published 10 June 2009)

We study with ^{17}O NMR and bulk magnetization a lightly electron doped $CaMnO_{3-x}$ ($x<0.01$) polycrystalline sample in the *G*-type antiferromagnetic state. The ^{17}O NMR spectra show two lines with very different intensities corresponding to oxygen sites with very different local magnetic environments. The more intense unshifted line is due to the antiferromagnetic (AF) matrix. The thermal dependence of the magnetic moment of the AF sublattice deduced from the ^{17}O linewidth is typical of insulating three-dimensional Heisenberg antiferromagnets. The less intense, strongly shifted line directly evidences the existence of ferromagnetic (FM) domains embedded in the AF spin lattice. The extremely narrow line in zero magnetic field indicates a nearly perfect alignment of the manganese spins in the FM domains which also display an unusually weak temperature dependence of their magnetic moment. We show that these FM entities start to move above 40 K in a slow-diffusion regime. These static and dynamic properties bear a strong similarity with those of a small size self-trapped magnetic polaron.

DOI: 10.1103/PhysRevB.79.214414 PACS number(s): 75.25.+z, 75.47.Lx, 76.60.Es, 76.60.Jx

I. INTRODUCTION

The effect of doped electrons in an antiferromagnetic (AF) spin lattice of magnetic compounds with mixed valency was raised in the early 1960s by de Gennes.[1] A homogeneous canted AF phase was predicted with double exchange interaction between the mobile electrons and the magnetic ions when extra electrons are added to a pure AF insulator. It was shown later that in doped manganites a homogeneous canted AF state should be unstable with respect to a electron phase separation.[2] In particular, at low doping, the AF lattice of localized spins should coexist with microsize areas of a modified phase[3] referred to as magnetic polarons (MPs).[4,5] The MP contains one electron "dressed" with a ferromagnetic (FM) polarized cloud of neighboring magnetic ions.

The MP can be bound or self-trapped. In the bound magnetic polaron concept the extra electron is bound by the Coulomb potential near defects and polarizes its neighboring localized magnetic moments. The mobility of the bound MP has an activated behavior with an activation energy E_a defined by the position of the donor level within the band gap. For the self-trapped magnetic polaron (STMP) the dressed electron is mainly stabilized by the exchange interaction with the ionic spins. As noted by de Gennes:[1] "the three-dimensional (3D) alternated AF spin lattice (i.e., a *G*-type AF) should restrict the mobility of electrons favoring for each individual carrier to build up a local distortion of the spin lattice in which the electron becomes self-trapped."

In view of this, the origin of the weak FM moment observed in bulk magnetization of the AF phase of lightly electron-doped manganites should be clarified. $CaMnO_3$ has a nearly cubic crystal structure of Mn^{+4} ions[6,7] and a *G*-type AF order appears together with a weak FM moment below $T_N \sim 120$ K.[8] Small-angle elastic-neutron-scattering[9] studies show the existence of local FM regions (~ 10 Å) in $Ca_{1-x}La_xMnO_3$ ($x=0.02$) while results of transport and magnetization[10] are attributed to the formation of MPs with a binding energy $E_b \sim 100$ meV and displaying an activated behavior of the conductivity. The existence of MP in lightly oxygen deficient $CaMnO_{3-x}$ is an open question. In lightly doped $SrMnO_{3-x}$ and $CaMnO_{3-x}$ low-temperature transport data are described as the formation of small size bound MPs in $SrMnO_{3-x}$ whereas in $CaMnO_{3-x}$ it is rather suggested to consider a Dzyaloshinsky-Moriya (DM) coupling as the origin of the weak FM moment.[11] On the other hand a theoretical study of the MP formation suggests to consider small size STMPs in lightly doped $CaMnO_{3-x}$ and shows that the STPM hopping requires an intermediate spin configuration associated to an energy barrier of $E_a \sim 40$ meV.[12]

The bulk magnetization data, M, showing a small FM contribution below T_N cannot trace unequivocally the properties of FM entities inside the sample since M may also include a FM contribution due to a zero-field spin canting of the AF structure as the DM coupling[13] is allowed by the symmetry in $CaMnO_3$. Thus, local informations are required to evidence and study any magnetic entity embedded in the AF matrix.

In this paper we present ^{17}O NMR and bulk magnetization studies of the magnetic inhomogeneity in the AF phase of a $CaMnO_{3-x}$ polycrystalline sample. The sample is lightly doped with electrons due to a small amount of oxygen vacancies ($x<0.01$) inherently existing in perovskite oxides.[11,14] In manganites the magnetic local field on the ^{17}O nuclei, h_{loc}, originates from the classic dipolar and from the transferred hyperfine interactions of the nuclear spin ^{17}I with the electron spin S of the neighboring Mn ions. The direction and magnitude of h_{loc} depend on the mutual orientations and on the thermal average value $\langle S \rangle$ so that h_{loc} at ^{17}O is a very

sensitive local probe of static and time fluctuating spin correlations of the neighboring Mn ions.[15,16] Our ^{17}O NMR data evidence directly the existence of small FM entities in the AF matrix. Due to their static and dynamic characteristics these FM entities are interpreted as small size self-trapped MPs.

II. EXPERIMENTAL DETAILS

The ceramic sample of $CaMnO_3$ was prepared by chemical homogenization technique. Water solutions of metal nitrates were mixed in the proper molar ratio. Ash-free paper filters were soaked with the solution then dried at 110 °C and burned. The residue was annealed 1 h at 600 °C in air and pressed into pellets. The final annealing was done at 1200 °C for 16 h in air. The sample was very slowly cooled down to room temperature in the oven.

The pellet was crushed into powder with an average grain size ~15 μm and enriched by ^{17}O up to ~15 at. % ^{17}O by conditioning at 930 °C for 140 h in an oxygen gas flow ($P_{O_2} \approx 1.5$ bar) with a subsequent slow cooling with the furnace. X-ray powder diffraction at room temperature shows that the ^{17}O-enriched sample is almost single phase with an orthorhombic structure and negligible inclusions of nonmagnetic CaO (<1 wt %). The unit-cell parameters determined in the *Pnma* space group are $a=5.2786(6)$ Å, $b=7.4508(10)$ Å, and $c=5.2670(6)$ Å. These values are in the range of the structural parameters quoted for the nearly stoichiometric oxide $CaMnO_{3-x}$ ($x<0.02$).[6,7,17–19] In the orthorhombic structure of $CaMnO_3$ the oxygen atoms have no inversion symmetry and two sites O(1) and O(2) are present with a slightly different Mn-O-Mn bond angle, 154(2)° for O1 site and 157(2)° for O2 as deduced from our x-ray data and the atomic positions of Ref. 6.

III. RESULTS AND DISCUSSION

A. SQUID magnetization

The temperature dependence of $M(T)$ in zero-field-cooled (M_{ZFC}) and field cooled (M_{FC}) runs, measured with a superconducting quantum interference device (SQUID) magnetometer in the magnetic fields $H=1$; 50 kOe are shown in Figs. 1(a) and 1(b). The $M(T;H)$ behavior is quantitatively very close to the results reported for nominally stoichiometric $CaMnO_{3-x}$ ($x<0.01$).[6,14,19–21] $M_{FC}(T)$ clearly shows a FM component that appears just below the Neel temperature, $T_N=123(1)$ K, defined as the position of the cusp in $M_{ZFC}(T)$ curve. Above 200 K the magnetic susceptibility M/H demonstrates the mean-field behavior $\sim(T-\theta)^{-1}$ with a negative paramagnetic Weiss temperature $\theta \approx -380$ K, indicating that AF spin correlations dominate between Mn neighbors in the paramagnetic phase. The linear fit of H/M data [inset in Fig. 1(b)] yields for the effective magnetic moment $\mu_{eff}=3.9(4)\mu_B$ per Mn very close to the value expected for $Mn^{4+}(S=3/2,\ L=0)$ ion in the pure spin state.

The isothermal behavior of M vs H was studied from 2 to 140 K. The isotherm at $T=40$ K is shown in Fig. 1(c). The hysteresis loop is the sum of two contributions:

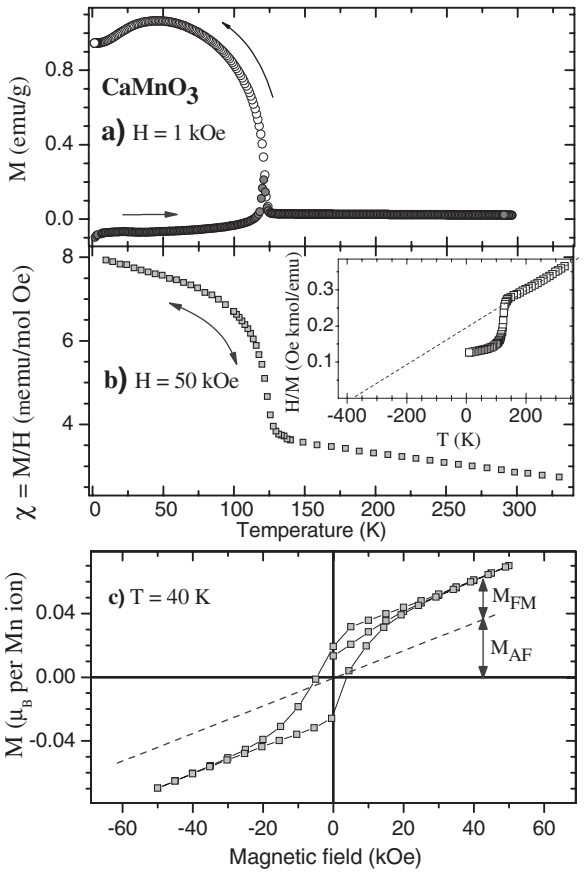

FIG. 1. Magnetization (a) M and (b) $\chi=M/H$ versus temperature measured at $H=1$ and 50 kOe, respectively, for $CaMnO_{3-x}$ ($x<0.01$) sample. Inset of (b): H/M versus temperature, the dashed line is a linear fit above 200 K. (c) M versus H measured at $T=40$ K. M_{AF} and M_{FM} are explained in the text.

$$M(H) = M_{AF} + M_{FM}. \quad (1)$$

The first contribution is due to the AF structure uniformly polarized by the external field. This contributes by a linear increase in M_{AF} with H since the variation in the angle of the AF-ordered magnetic moments of Mn is less than 1° in the range of our magnetic fields.

At high fields the vertical distance between $M(H)$ and M_{AF} determines the M_{FM} contribution which appears to be constant. Thus the M_{FM} contribution saturates at $H>20$ kOe. M_{FM} may be interpreted in two ways. First, M_{FM} is considered as due to small FM domains. Following the idea[14] that M_{FM} is due to [Mn^{3+}-(O-vacancy)-Mn^{3+}] clusters, we estimate from M_{FM} the upper limit of the O vacancies content as $x<0.01$ in our sample (assuming the minimal size ~$2a$ of the FM domain). Second, M_{FM} is attributed to a zero-field spin-canted AF structure due to the DM coupling. In that case the resulting phase is homogeneous in contrast to the first interpretation. Finally both contributions may coexist. Nevertheless, in a lightly doped $Ca_{1-x}La_xMnO_3$ with $x=0.02$ the FM contribution seen by neutron diffraction and magnetization was attributed to nanometric FM clusters excluding a homogeneous spin-canted state at this low doping.[9]

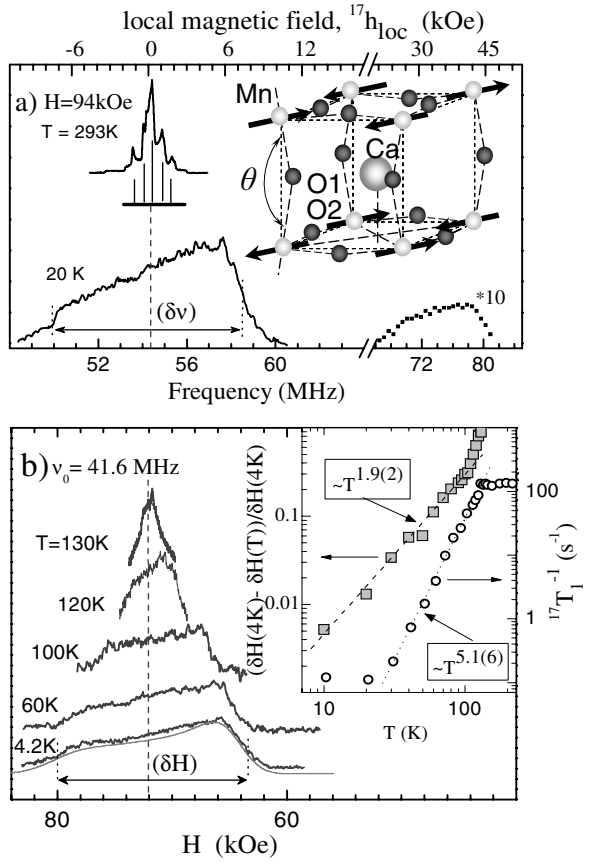

FIG. 2. ^{17}O NMR spectra measured (a) at $H=94$ kOe with frequency sweep in the paramagnetic and AF states and (b) at $\nu_0=41.6$ MHz with field sweep. At 4.2 K the spectrum is shown along with the fit for $\theta=154°$ (see text). The orthorhombic structure is schematically represented in (a). Inset of (b), AF phase: T dependences of the linewidth (δH) plotted as $[\delta H(4\text{ K})-\delta H(T)]/\delta H(4\text{ K})$ and of the spin-lattice relaxation rate T_1^{-1}. The dashed and dotted lines are the corresponding fits (see text).

B. ^{17}O NMR in the antiferromagnetic matrix

The ^{17}O NMR spectra shown in Fig. 2 were obtained (a) with frequency sweep at constant magnetic field $H=94$ kOe and (b) with field sweep at constant frequency $\nu_0=41.6$ MHz. ^{17}O nucleus has a spin $I=5/2$ and above T_N the interaction of the ^{17}O quadrupole moment $e^{17}Q$ with the electric field gradient (EFG) eV_{ii} of the charge environment[22] determines the spectrum pattern with five well resolved peaks of $2I$ transitions. These features are clearly seen in the spectrum for $T=293$ K on Fig. 2(a). The EFG tensor components $\nu_Q \equiv 3e^2QV_{ZZ}/2I(2I-1)=930(16)$ kHz for both O sites and $\eta \equiv |(V_{XX}-V_{YY})/V_{ZZ})|$ is 0.05 for O2 and a little bit larger for O1 site. All the components are temperature independent in the paramagnetic phase. In the AF state where the quadrupolar structure of the spectrum is completely smeared by the magnetic interactions we used the same EFG parameters in the analysis of ^{17}O NMR spectra. Below $T_N=123$ K the spectrum splits in two broad lines with very different resonance frequencies and intensities as shown for $T=20$ K on Fig. 2(a).

The main line is close to Larmor frequency ν_0 and evidently originates from oxygens in the AF matrix of $CaMnO_3$. It shows an asymmetric trapeziumlike shape whose linewidth, $\delta\nu=\gamma\delta H$ (where γ is the ^{17}O gyromagnetic ratio), can be well estimated with the classic dipolar fields created by the Mn^{+4} magnetic moments at the oxygen sites. The NMR powder pattern is calculated in the frozen G-type spin lattice. We used $\mu_{staggered}(Mn^{+4})=2.8\mu_B$ (Ref. 21) and our Mn-O distances whereas the Mn-O-Mn bond angle was the only fitting parameter. This calculated line shape for both O1 and O2 sites is finally convoluted with the broadening function describing the quadrupole-splitted spectrum in the paramagnetic phase. The result for 154° is shown in Fig. 2(b) by the gray curve for $T=4.2$ K. The quantitative consistency between the optimal fitting value of the Mn-O-Mn bond angle and that obtained from structural data allows us to ignore the short-range hyperfine transferred interactions which dominates in the Mn^{+3}/Mn^{+4} mixed-valence manganites.[15,16,23] Since the dipolar width δH is proportional to the average Mn magnetic moment in a AF sublattice its temperature dependence is the one of the sublattice magnetization.

The T dependence of (δH) is shown in the inset of Fig. 2(b) as the dimensionless ratio $[\delta H(4\text{ K})-\delta H(T)]/\delta H(4\text{ K})$. The exponent $\alpha=1.9(2)$ of the T^α power law is a signature of antiferromagnets with an isotropic Heisenberg exchange ($\alpha_{theor}=2$).[24] The same conclusion follows from the temperature dependence of the nuclear-spin-lattice relaxation rate, $T_1^{-1}(T)$, which probes the low-frequency dynamics of the AF spin lattice. In the same inset the drop of T_1^{-1} in 3 orders of magnitude from T_N down to $T_N/5\sim 20$ K is well fitted with a power law $T_1^{-1}\sim T^{5.1(5)}$ consistent with the T^5 dependence of $T_1^{-1}(T)$ due to a three-magnons scattering process in isotropic AF insulators.[24]

C. ^{17}O NMR in the ferromagnetic domains

In total contrast the less intense line is largely shifted toward high frequency so that the main interaction to be considered for this signal cannot be the same as for oxygen in the AF matrix. This line is in the same frequency range as the ^{17}O NMR line due to oxygens in the FM domains of the half-doped manganites, e.g., $Nd_{0.5}Sr_{0.5}MnO_3$ (FM phase) (Ref. 23) and $Pr_{0.5}Ca_{0.5}MnO_3$ (FM domains in the H-melted CO state).[16] Moreover its intensity is about 3% of the total NMR spectrum which is in a reasonable agreement with a simple electroneutrality consideration. Each oxygen vacancy (one removed O^{2-} ion) leads to a corresponding decrease in the positive charge of the Mn-ions sublattice.[14] As a consequence for x oxygen vacancies the valence state of at least $2x$ Mn ions is changed from $Mn^{4+}(t_{2g}^3e_g^0)$ to a more magnetic state with a partially filled e_g orbital. These Mn ions nucleate FM domains inside the AF spin lattice of $CaMnO_3$ and their magnetization contributes to the bulk magnetization data below T_N (Fig. 1).

For doped manganites the large h_{loc} value at oxygen sites originates from the Fermi contact interaction of the nuclear spin ^{17}I with the transferred s-spin density of electrons due to the overlap of the $O(2s2p_\sigma)$ and $Mn(e_g)$ orbitals:[15,25]

$$\boldsymbol{h}_{loc}(2s)=2f_sH_{FC}(2s)\langle \boldsymbol{S}\rangle, \quad (2)$$

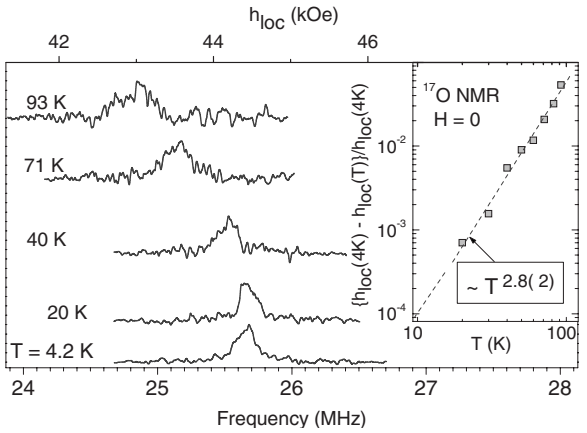

FIG. 3. ^{17}O zero-field NMR spectra measured in the FM domains of $CaMnO_{3-x}$. Inset: T dependence of $[h_{loc}(4\ K) - h_{loc}(T)]/h_{loc}(4\ K)$, the dotted line is a power-law fit (see text).

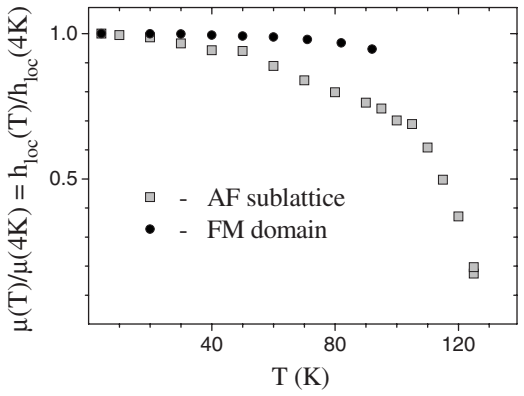

FIG. 4. Temperature dependences of $h_{loc}(T)/h_{loc}(4\ K) = \mu(T)/\mu(4\ K)$ for the FM domains and for the AF sublattice in $CaMnO_{3-x}$.

where $H_{FC}(2s)$ is the hyperfine magnetic field produced by one unpaired electron on the O $2s$ orbital. The corresponding s-wave spin density transferred from two Mn neighbors is defined as $f_s = h_{loc}(2s)/H_{FC}(2s)$ for 1 μ_B effective moment of the magnetic ion. Finally, $\boldsymbol{h}_{loc} \sim \langle \boldsymbol{S} \rangle \sim \langle \vec{\mu} \rangle$.

In contrast to NMR ($H \neq 0$) in zero-field NMR the broadening of a spectrum by the demagnetizing fields in polycrystalline samples is absent so that the intrinsic distribution of h_{loc} due to various orientations of the magnetic moments inside the FM domains can be studied. The zero-field ^{17}O NMR spectrum at $T=4.2$ K measured in the frequency range $\nu=(15-35)$ MHz shows a very narrow line $\delta\nu_{FM} \sim 0.2$ MHz (Fig. 3) peaked near $\nu=25.7$ MHz ($h_{loc}=44$ kOe). This value is consistent with the frequency position of the less intense broad line detected at $H=94$ kOe [Fig. 2(a)] so that both lines, at $H=0$ and 94 kOe, originate from the same oxygen atoms in the FM domains.

The resonance frequency ν of an oxygen is defined by the magnitude of the vector sum $\boldsymbol{h}_{loc}$ from its two Mn neighbors. Furthermore the width of the zero-field line, $\delta\nu_{FM}$, is sensitive to both the magnitude and the mutual alignment of the Mn spins. The small value of the ratio $\delta\nu_{FM}/\nu=0.01$ demonstrates a nearly perfect alignment of the Mn spins in the FM domains. Remarkably, the line does not show the quadrupole splitting. The principal axis $\boldsymbol{OZ}$ of the EFG tensor corresponds to its V_{ZZ} component and is roughly directed along the axes of the pseudocubic unit cell.[26] The absence of quadrupole splitting is interpreted as due to the fact that the angle between $\boldsymbol{h}_{loc}$, the quantization axis, and $\boldsymbol{OZ}$ is close to the "magic angle" $\sim 54°$, thus the [111] direction is favored for the Mn magnetic moment $\langle \vec{\mu} \rangle_{FM}$ in the FM domains.

It should be emphasized that the thermal variation in $h_{loc}(T)/h_{loc}(4\ K)$ measured up to $\sim 4/5\ T_N$ is unusually small for FM domains. For comparison in Fig. 4 is also plotted the temperature dependence of the AF sublattice moments as the ratio $\mu(T)/\mu(4\ K) = h_{loc}(T)/h_{loc}(4\ K)$. Besides, the T^α fit of $[h_{loc}(4\ K) - h_{loc}(T)]/h_{loc}$ vs T yields $\alpha=2.8(2)$ as shown in the inset of Fig. 3. This value is very different from the $T^{3/2}$ Bloch law expected for $M(T)$ in macroscopic FM domains. It is known that for FM domains smaller than 100 nm the acoustic magnon branches providing the main contribution to the Bloch law are modified.[27] This fact is in support of small size FM domains in our sample.

The almost temperature independence $\langle \mu \rangle_{FM}$ and the nearly perfectly aligned Mn spins in a wide T range allow us to consider the FM domains as saturated which is a signature of a small size MP.[12,28] It is worth noting that the value of the transferred spin polarization $f_s\langle S \rangle = 0.05\langle S \rangle$ at O($2s$) orbital inside the MP is the same as the one obtained for oxygen in the metallic FM phase of $Nd_{0.5}Sr_{0.5}MnO_3$.[23] By analogy we suggest to consider a similar mechanism implying a rather strong O($2s2p_\sigma$)-Mn(e_g) hybridized state for the electron in the MP.

The low-frequency dynamics of the Mn spins was studied in both the MPs and the AF matrix by measuring the ^{17}O spin-echo-decay rate, T_2^{-1}, on the zero-field NMR line (in MPs) and on the NMR line (AF matrix). The echo-decay data were collected using the conventional $(\pi/2 - t - \pi - t)$—echo pulse sequence. The characteristic time of the echo decay, T_2, is defined as the time at which the echo signal $E(2t)$ drops to $1/e$ of its starting value. In both cases T_2^{-1} is almost constant from 4 to 40 K and increases above 40 K so that at $T>93$ K the FM signal is lost due to too short T_2. The component $(T_2^{-1})_a$ defined as $(T_2^{-1})_a \equiv [T_2^{-1}(T) - T_2^{-1}(4\ K)]$ shows a thermal activated behavior $\sim \exp(E_a/k_BT)$ with $E_a=180(20)$ K ~ 15 meV as shown in the inset of Fig. 5 for the MPs.

It is remarkable that in the same temperature range where the $(T_2^{-1})_a$ term is clearly seen, an electron-transport study of a $CaMnO_3$ single crystal[11] with an oxygen deficiency comparable to our sample shows that the bound electron becomes mobile. In the MP scenario the electron should move from site to site with its FM polarized surrounding thus creating time-dependent spin fluctuations with a correlation time τ_c related to the MP mobility.

Let us analyze $(T_2^{-1})_a$ in the MPs. In general, the time-dependent fluctuations of the local-field components i.e., the transverse, $h_\perp$, and the longitudinal, $h_\parallel$, components contribute to the echo-decay process.[22] In contrast, the nuclear-spin-lattice relaxation rate, T_1^{-1}, involves only the transverse components of the fluctuating field and probes $\langle h_\perp(0)h_\perp(t) \rangle$. We measured T_1 and find that in the whole temperature range $T_1^{-1} < 0.001 T_2^{-1}$. This permits to consider $\langle h_\parallel(0)h_\parallel(t) \rangle$

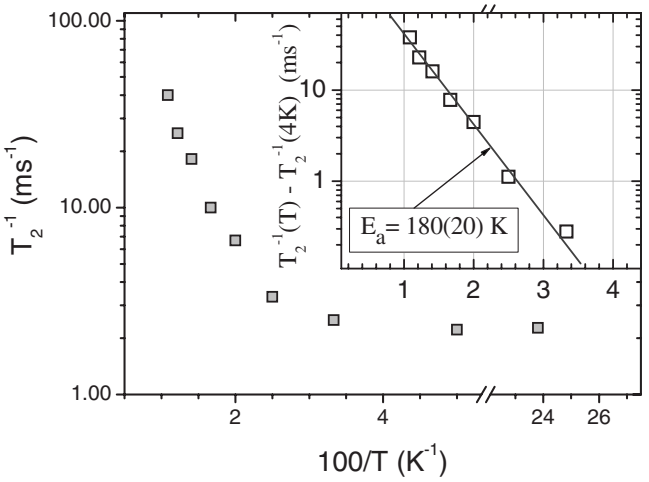

FIG. 5. ^{17}O spin-echo-decay rate T_2^{-1} vs T^{-1} measured in zero-field NMR in the FM domains of $CaMnO_{3-x}$. The inset shows the activated component $[T_2^{-1}(T) - T_2^{-1}(4\ \mathrm{K})]$ versus $1/T$.

$= h_{\|}(0)^2 \exp(-t/\tau_c)$ as the main contribution to $(T_2^{-1})_a$. A ^{17}O nucleus captured inside the MP has a resonance frequency $\nu = \nu_{\mathrm{FM}} = \gamma h_{\mathrm{loc,FM}}$. When the MP moves away, ν changes immediately to $\nu_{\mathrm{AF}} = \gamma h_{\mathrm{loc,AF}} \sim \gamma(\delta H)_{\mathrm{AF}}$ for this oxygen spin which contributes no more to the echo signal. The very small change with T of ν_{FM}, $[\nu_{\mathrm{FM}}(4\ \mathrm{K}) - \nu_{\mathrm{FM}}(T)]/\nu_{\mathrm{FM}}(4\ \mathrm{K}) < 0.05$, indicates that up to ~ 100 K the MPs are in the slow-diffusion regime, i.e., $\tau_c \Omega \gg 1$ where $\Omega = \gamma(h_{\mathrm{loc,FM}} - h_{\mathrm{loc,AF}}) \sim \gamma h_{\mathrm{loc,FM}}$, whereas for fast-diffusing MPs with $\tau_c \Omega \ll 1$ one should expect a strong shift of the resonance frequency ν_{FM} toward ν_{AF} as the temperature rises. In the slow-fluctuations regime the echo decay takes a simple exponential form $E(2t) \sim \exp\{-2t/T_2\}$ with $T_2 = \tau_c$.[22,29] Thus $(T_2^{-1})_a$ data permit a direct measure of τ_c, the MP hopping correlation time.

IV. CONCLUSION

In conclusion, the ^{17}O NMR study of a lightly electron doped $CaMnO_{3-x}$ with $x < 0.01$ evidences that FM domains are embedded in the G-type AF spin lattice. This does not exclude a contribution of the Dzyaloshinsky-Moriya coupling to the M_{FM} term of the bulk magnetization. The nature of the interaction of the ^{17}O spin with its neighboring Mn spins is very different in the AF matrix and in the FM domains. The properties studied in the matrix indicate that it behaves as a 3D Heisenberg antiferromagnet. In the FM domains we find from ^{17}O linewidth that the Mn spins are perfectly aligned as expected for MPs and from the line shift that the e_g electron is responsible for the ^{17}O local field through the $O(2s2p_\sigma)$-$Mn(e_g)$ hybridized state. Furthermore the almost temperature independence of the magnetic moment in the FM domains together with the thermally activated spin dynamics with $E_a \sim 15$ meV agree with the model of small size self-trapped magnetic polarons[12] and as $E_a \ll E_b \sim 100$ meV the stability of the MP is ensured when it moves through the AF spin lattice. Indeed, according to the ^{17}O echo-decay data the MP starts to move above 40 K keeping its static properties almost unchanged.

ACKNOWLEDGMENTS

This work was supported in part by the Russian Foundation for Basic Research under Grants No. 06-02-17386, No. 08-02-00029, and No. 09-02-00310. S.V., A.G., and A.Y. are grateful to ESPCI and CNRS for hospitality and support.

[1] P.-G. de Gennes, Phys. Rev. **118**, 141 (1960).
[2] A. Moreo, S. Yunoki, and E. Dagotto, Science **283**, 2034 (1999).
[3] E. Nagaev, JETP Lett. **6**, 484 (1967).
[4] T. Kasuya, A. Yanase, and T. Takeda, Solid State Commun. **8**, 1543 (1970).
[5] N. Mott, *Metal-Insulator Transitions* (Taylor and Francis, London, 1974), p. 270.
[6] I. Fawcett, J. Sunstrom, M. Greenblatt, M. Croft, and K. Ramanujachary, Chem. Mater. **10**, 3643 (1998).
[7] K. R. Poeppelmeier, M. E. Leonowicz, J. C. Scanlon, J. M. Longo, and W. B. Yelon, J. Solid State Chem. **45**, 71 (1982).
[8] E. O. Wollan and W. C. Koehler, Phys. Rev. **100**, 545 (1955).
[9] E. Granado, C. D. Ling, J. J. Neumeier, J. W. Lynn, and D. N. Argyriou, Phys. Rev. B **68**, 134440 (2003).
[10] J. J. Neumeier and J. L. Cohn, Phys. Rev. B **61**, 14319 (2000).
[11] C. Chiorescu, J. L. Cohn, and J. J. Neumeier, Phys. Rev. B **76**, 020404(R) (2007).
[12] H. Meskine and S. Satpathy, J. Phys.: Condens. Matter **17**, 1889 (2005).
[13] I. Dzyaloshinsky, J. Phys. Chem. Solids **4**, 241 (1958).
[14] J. Briatico, B. Alascio, R. Allub, A. Butera, A. Caneiro, M. T. Causa, and M. Tovar, Phys. Rev. B **53**, 14020 (1996).
[15] A. Yakubovskii, A. Trokiner, S. Verkhovskii, A. Gerashenko, and D. Khomskii, Phys. Rev. B **67**, 064414 (2003).
[16] A. Trokiner, A. Yakubovskii, S. Verkhovskii, A. Gerashenko, and D. Khomskii, Phys. Rev. B **74**, 092403 (2006).
[17] Z. Zeng, M. Greenblatt, and M. Croft, Phys. Rev. B **59**, 8784 (1999).
[18] Y. Moritomo, A. Machida, E. Nishibori, M. Takata, and M. Sakata, Phys. Rev. B **64**, 214409 (2001).
[19] C. D. Ling, E. Granado, J. J. Neumeier, J. W. Lynn, and D. N. Argyriou, Phys. Rev. B **68**, 134439 (2003).
[20] C. Chiorescu, J. J. Neumeier, and J. L. Cohn, Phys. Rev. B **73**, 014406 (2006).
[21] C. R. Wiebe, J. E. Greedan, J. S. Gardner, Z. Zeng, and M. Greenblatt, Phys. Rev. B **64**, 064421 (2001).
[22] C. Slichter, *Principles of Magnetic Resonance* (Springer-Verlag, Berlin, 1990), p. 640.
[23] A. Trokiner, S. Verkhovskii, A. Yakubovskii, K. Kumagai, P. Monod, K. Mikhalev, A. Buzlukov, Y. Furukawa, N. Hur, and S.-W. Cheong, Phys. Rev. B **77**, 134436 (2008).
[24] E. Turov and M. Petrov, *Nuclear Magnetic Resonance in Ferro- and Antiferromagnets* (Halsded, New York, 1972), p. 207.

[25] The contribution $h_{\mathrm{loc}}(2p)$ to the local field at oxygen sites was not considered since $h_{\mathrm{loc}}(2p)$ is smaller than $h_{\mathrm{loc}}(2s)$ by more than 1 order of magnitude. $h_{\mathrm{loc}}(2p)$ arises from a transferred polarization on the $\mathrm{O}(2p)$ orbital due to the $\mathrm{O}(2p_\sigma)$-$\mathrm{Mn}(t_g)$ orbital overlap.

[26] N. Medvedeva (unpublished).

[27] A. Akhiezer, V. Bar'Yakhtar, and S. Peletminskii, *Spin Waves* (North-Holland, Amsterdam, 1968), p. 268.

[28] A. J. Millis, Phys. Rev. B **55**, 6405 (1997).

[29] J. Witteveen, Phys. Rev. B **55**, 8083 (1997).